# Density Functional Theory Calculations of the Structures, Binding Energies, and Infrared Spectra of Methanol Clusters

**Fredrick C. Hagemeister, Christopher J. Gruenloh, and Timothy S. Zwier***

*Department of Chemistry, Purdue University, West Lafayette, Indiana 47907-1393*

*Received: November 12, 1996; In Final Form: August 11, 1997*[⊗]

Density functional theory (DFT) calculations of the structures, binding energies, vibrational frequencies and infrared intensities of methanol clusters containing two to five molecules have been carried out using the Becke3LYP functional. Thirteen representative H-bonded structures have been studied including cyclic, chain, branched-cyclic and branched-chain hydrogen bond structures. In the methanol trimer, tetramer, and pentamer, the cyclic structure is more stable by 3.5, 8.3, and 3.6 kcal/mol over the next most strongly bound minimum. In the tetramer and pentamer, the second-most stable minimum corresponds to a branched cycle. Chain structures are destabilized from the cyclic minimum by the loss of a hydrogen bond and from a smaller cooperative strengthening of the H-bonds that remain. In all branched structures studied, the formation of the branch H-bond strengthens the "branch-point" methanol's H-bond donation to its neighbor, but weakens its two acceptor H-bonds, leading to largely compensating effects on the total binding energy. The computed OH stretch vibrational frequency shifts (relative to the monomer at the same level of calculation) are used as points of comparison with recent experimental work on gas-phase $(methanol)_m$ and benzene−$(methanol)_m$ clusters and matrix-isolated $(methanol)_m$ clusters.

## I. Introduction

Molecular clusters serve as an important testing ground for current intermolecular potentials of hydrogen-bonded molecules.[1−3] In $(ROH)_n$ clusters, each OH group possesses one donor and two acceptor sites for H-bonds, leading to an exponentiating number of minima in the intermolecular potential energy surface with increasing cluster size. Since cooperative effects are sensitively dependent on the number, strength, and orientation of the hydrogen bonds present,[1,4] a reliable foundation of experimental and computational results on various H-bonded cluster structures is clearly needed to test current potentials. The experimental challenge is to make these isomers, distinguish them from one another, and determine their unique spectral signatures.[5−12] The theoretical challenge is to predict structures, binding energies, vibrational frequencies,[4,13−16] tunneling splittings, and tunneling pathways[17−21] for these clusters with sufficient accuracy to guide and interpret the experimental data and ultimately refine the existing intermolecular potentials[1,3] used in simulations of hydrogen-bonded liquids and solids.

In the study of methanol clusters, recent experimental progress is being made on several fronts. Studies of pure, gas-phase methanol clusters[5,22−28] in the microwave and infrared have provided spectral evidence for the lowest-energy structures of methanol clusters with $m = 2-5$. The microwave spectrum of the methanol dimer[25,27] reveals a donor/acceptor structure very much like that of the water dimer.[29−31] Infrared data in the CO stretch[5,22] and OH stretch[23] regions are also available, including measurements of the absolute cross sections for the donor and acceptor OH stretch fundamentals.[23] The gas-phase methanol clusters with $m > 2$ are thought to be H-bonded cycles.[5,22−26] The CO stretch[5,22] and OH stretch[28] infrared spectra of the methanol trimer are consistent with a cyclic structure, again as in the water trimer.[32−34] The tetramer and pentamer data,[5,22,23] while considerably more sparse, nevertheless also point to a preference for cyclic structures in the cold, supersonic expansion. Finally, CO stretch infrared spectra of the methanol hexamer have been analyzed in terms of an $S_6$ cyclic structure which, under warmer expansion conditions, undergoes a transition to a $C_2$ cyclic boat structure.[5,35]

Our group has recently obtained size-specific OH stretch infrared spectra of cold, gas-phase benzene−$(methanol)_m$ clusters with $m = 1-6$ using resonant ion-dip infrared spectroscopy.[36] In this case, complexation of benzene to the $(methanol)_m$ clusters provides a means of size- and conformation selection while at the same time probing the effects of benzene on the $(methanol)_m$ clusters. The sensitivity of the OH stretch vibrational frequencies and intensities to the hydrogen-bonding environment make the OH stretch infrared spectrum an especially powerful probe of the hydrogen-bonding topology of the clusters.[12,37]

Finally, a wider range of hydrogen-bonded structures for the methanol clusters have been formed and studied recently in a nitrogen matrix by Coussan et al.[38,39] Using a combination of thermal annealing, concentration changes, infrared-induced isomerization, and infrared hole-burning, these authors have identified O−H stretch, C−H stretch, and C−O stretch infrared transitions due to cyclic and open-chain trimers, and methanol tetramers which are cyclic, branched-cyclic, and branched-chain.

Given this recent influx of new experimental data, computed structures, binding energies, and particularly OH stretch vibrational frequencies and intensities are needed for a wide range of $(methanol)_m$ and benzene−$(methanol)_m$ cluster structures. In our previous report on benzene−$(methanol)_m$ clusters,[36] density functional theory (DFT) calculations were used as a basis for distinction among the possible hydrogen-bonded structural types observed experimentally, but an analysis of the calculated structures, binding energies, and OH stretch normal modes was not taken up. Such an analysis is given here. We also present a more detailed account of the benzene−$(methanol)_m$ calcula-

* To whom correspondence should be addressed.
[⊗] Abstract published in *Advance ACS Abstracts,* December 1, 1997.

S1089-5639(96)03763-2 CCC: $15.00 
Published on Web 01/01/1998

tions which serve as a quantitative point of comparison with our experiments.

Several previous computational studies of methanol clusters have been conducted.[40−52] Much of this work has concentrated on the methanol dimer,[40−44] often with an eye towards producing a two-body, ab initio-based intermolecular potential for use in condensed phase simulations of methanol. Mo et al.[45,46] have recently carried out large basis set Hartree−Fock, MP2, and DFT/Becke3LYP calculations on the cyclic methanol trimer, including harmonic vibrational frequency calculations. Buck and Schmidt[53] have modified the perturbation approach of Buckingham[54−56] to calculate the vibrational frequencies of methanol clusters up through the hexamer. The reported results of that study concentrate on the CO stretch vibrations since these have received much attention from experiment.

In this work, calculations on a total of 13 minimum-energy structures of the pure methanol clusters are described. This representative set includes a single structure for the methanol dimer, three methanol trimer structures, five tetramer, and four pentamer structures. The range of structural types studied includes cyclic, chain, branched cyclic, and branched chain structures. Apart from the minimum basis set study of Curtiss et al.,[48] eight of these structures have not been studied before at any level of theory. The DFT calculations employ the Becke3LYP exchange-correlation functional,[57−59] in most cases using the 6-31+G* basis set. Special emphasis will be placed on a comparison of the calculated OH stretch vibrational frequency shifts and intensities with the recent experimental data on $(\text{methanol})_m$[5,22−28] and benzene−$(\text{methanol})_m$[36] clusters.

As an aid in referring to the various structures studied, the following short-hand notation will be used, generalized from that introduced by Buck and Schmidt.[53] An *n*-membered cycle and chain are given the symbols (n) and $\underline{\text{n}}$, respectively. Branched cycles and chains are then referred to as (n) + *m* or $\underline{\text{n}}$ + *m* where *m* refers to the number of methanols in the branch. In the case of branched chains, the point of attachment of the branch to the chain is given by a subscript on the branch. The numbering in the chain begins at the free OH end, and is included in the figures. Thus, the $\underline{3} + 1_2$ structure is a methanol tetramer composed of a trimer chain with a single methanol branch attached to the middle methanol in the trimer chain.

## II. Calculational Methods

Density functional calculations were carried out using the Gaussian 92/DFT[60] and Gaussian 94[61] suite of programs. The calculations employ the Becke3LYP nonlocal exchange correlation functional[61−63] which has been extensively used in studies of water and methanol clusters and tested against MP2 ab initio calculations.[45,64−71] The results presented here on the methanol dimer and trimer (Sections III, IV) confirm that the properties obtained with B3LYP/6-31+G* give structures and binding energies in good agreement with the large basis set MP2 results (MP2/VTZ(2df,2p)) of Bleiber and Sauer[42] and the very large basis set DFT calculations of Mo et al. (B3LYP/6-311++G(3df,2p)).[45] In addition, the OH stretch vibrational frequency shifts predicted by B3LYP/6-31+G* are in close agreement with experimental vibrational frequency shifts on $(\text{water})_n$, $(\text{methanol})_m$, benzene−$(\text{water})_n$, and benzene−$(\text{methanol})_m$ clusters[36,72,73] which serve as the major point of comparison with recent experiments. In the benzene−$(\text{water})_n$ clusters, this agreement extends to cyclic, cage, and cubic structures up through the water octamer.[72,73] Since the present study seeks to identify the infrared spectral signatures of a variety of H-bonding topologies in the methanol clusters, the Becke3LYP/6-31+G* level of theory was chosen for much of our work. This basis set also allowed a seamless comparison with calculations on benzene−$(\text{methanol})_m$ clusters with $m = 2,3$ at the same level of theory. On the smaller methanol clusters, additional calculations using the 6-31+G′[2d,p] basis set were also carried out. The 6-31+G′[2d,p] basis set combines the standard 6-31+G(2d,p) basis set for the carbon atoms and the 6-31+G[2d,p] basis set for the O and H atoms. The 6-31+G-[2d,p] basis set is formed by combining the 6-31+G(2d,p) basis set with polarization functions from the aug-cc-pVDZ basis set,[74,75] and has been used previously in studies of water clusters and benzene−$(\text{water})_n$ clusters.[66]

The geometries of all 13 cluster structures considered were fully optimized. Most of the structures are local minima representative of a given hydrogen-bond topology (chain, branched chain, cyclic, or branched cyclic), as established by the absence of any negative vibrational frequencies. The reported structures are the lowest-energy minima of each structural type and cluster size. Other minima of the same structural type differ in the oxygen lone pair used for hydrogen bonding and in the orientation of the "dangling" methyl groups. In the cyclic and branched cyclic clusters, these local minima differ in the position of the methyl groups relative to the plane of the hydrogen-bonded ring. The lowest-energy cyclic structure has adjacent methyl groups alternating positions above and below the hydrogen-bonded plane, much as is the case for dangling hydrogens in $(H_2O)_n$.[1,4,64,76,77] In the less rigid chain structures, a larger number of alternate conformations exist. These differ in the oxygen lone-pairs chosen as H-bond acceptor sites and in the relative orientation of the methyl groups in the chain. The former choice dictates the secondary structure of the H-bonded chain as a curved, kinked, or zigzag H-bonded structure. For instance, in the methanol tetramer chain, the lone-pair connectivity of the three H-bonds produces 8 minima ($2^3$) which exist as four enantiomeric pairs with total binding energies of −24.02, −23.28, −22.50, and −22.27 kcal/mol. The present paper focuses attention only on the first of these. Future studies will be needed to determine the conditions under which conformational isomerization, either with or without tunneling, is significant.

Harmonic vibrational frequencies and infrared intensities have been calculated for all 13 structures. Only the OH stretch and selected C−O stretch vibrations, of particular relevance to experiment, are reported explicitly in the tables in the next section. The full set of vibrational frequencies and intensities are available from the authors upon request.

Total binding energies for the $(CH_3OH)_m$ clusters are calculated as

$$\text{BE} = E(\text{cluster}) - m{\cdot}E(\text{monomer})$$

where the monomer energy is determined at the same level of theory as the cluster. The negative of the binding energy gives the dissociation energy $D_e$. Zero-point corrections to $D_e$ using the harmonic vibrational frequencies are also made.

Corrections for basis-set superposition error (BSSE)[78] have been estimated for the dimer and all three of the trimer structures using the full counterpoise procedure. For the dimer, the BSSE correction is 1.12 kcal/mol at the 6-31+G* but only 0.36 kcal/mol with the 6-31+G′[2d,p] basis set. For the chain, cyclic, and "T" structures of the trimer the BSSE corrections for the binding energies calculated using the 6-31+G* basis set are 2.30, 2.42, and 2.12 kcal/mol, respectively. The BSSE corrections, although sizable with the 6-31+G* basis set, are similar for different structures and are relatively unimportant

for the relative stabilities. BSSE corrections to the binding energies of the nine tetramer and pentamer structures are less practical and have not been carried out.

## III. Results

The key structural parameters for the monomer and 13 methanol cluster structures using the 6-31+G* basis set are summarized in Table 1. The table includes those intramolecular and intermolecular parameters which are most affected by hydrogen bonding; namely, the OH bond distance ($r_{OH}$), the COH bond angle ($a_{COH}$), the oxygen−oxygen separation between H-bonded neighbors ($R_{OO}$), and the OH···O hydrogen bond angle. Changes in the O−O separation, $\Delta R_{OO}$, accompanying an increase in size or addition of a branch to a cluster are also reported in Table 1. The methanol molecule in the parent structure used in the comparison is given in parentheses in the table, using the methanol numbering in Figures 1−4. In the cyclic and branched cyclic structures, $\Delta R_{OO}$ is computed relative to the average $R_{OO}$ separation in the corresponding unbranched cyclic structure, since no good one-for-one correspondence between individual methanol molecules exists.

The H-bonded cyclic structures for the trimer, tetramer, and pentamer are shown as inserts in Figure 1a−c, while the chain structures for the dimer, trimer, and tetramer are presented in Figure 2a−c, respectively. The three branched-chain and four branched-cycle structures investigated in this work are displayed in Figures 3 and 4, respectively. Finally, the lowest-energy benzene−(methanol)$_2$ and benzene−(methanol)$_3$ structures are shown as insets in Figure 5a,b.

The binding energies for the structures shown in Figures 1−4 are collected in Table 2. Values are given both with and without zero-point energy correction. For the dimer and trimer structures, BSSE-corrected binding energies are also included, as are values computed with the larger 6-31+G′[2d,p] basis set. The OH stretch harmonic vibrational frequencies and infrared intensities are reported in Table 3. The frequency shifts of the OH stretch vibrations from the value calculated for the free monomer (at the same level of theory) are also given.

As an aid in assessing the degree of localization or delocalization of the OH oscillators in a given OH stretch normal mode, the calculated OH stretch normal modes have been projected onto the basis set provided by the individual OH bond displacements of the methanol subunits. The fractional character of the normal modes in this local mode basis are given in Table 4, together with a sign indicating the relative phases of the OH oscillations in the mode.

Finally, Tables 5 and 6 provide a comparison of the results of the present calculations with both experimental and previous theoretical studies of the structures, binding energies, and vibrational frequency shifts of selected methanol clusters.

## IV. Discussion

**A. The Methanol Dimer and Benzene−(Methanol)$_2$.** The minimum-energy structure calculated for the methanol dimer is composed of H-bond donor and acceptor molecules bound in a near-linear H-bond (Figure 2a). Previous experimental and recent theoretical studies on the dimer are included in Tables 5 and 6 for comparison with the present results. In the dimer, the computed O−O separation from the present DFT calculations with the 6-31+G* and 6-31+G′[2d,p] basis sets are 2.862 and 2.881 Å, respectively. We have corrected the calculated equilibrium distance for vibrational averaging by fitting the one-dimensional methanol-methanol stretching potential to a power series in $R_{OO}$, and subsequently determining the $v = 0$ $\langle R_{OO} \rangle$ using the Numerov procedure.[79] The corrected values are 2.880 and 2.904 Å, respectively, compared to an experimental value[27] for $\langle R_{OO} \rangle$ of 2.98 Å. The comparison with other calculated values are shown in Table 5.

**TABLE 1: Key Structural Parameters for the Methanol Cluster Theoretical Structures Studied Herein**[a]

| | MeOH unit[b] | $r_{OH}$ | $a_{COH}$ | $R_{OO}$[c] | $\Delta R_{OO}$[d] | $a_{OHO}$[c] |
|---|---|---|---|---|---|---|
| $(MeOH)_1$ | 1 | 0.969 | 109.2 | | | |
| $(MeOH)_2$ | 1 | 0.969 | 109.4 | | | |
| 2 | 2 | 0.977 | 109.3 | 2.862 | | 174.2 |
| $(MeOH)_3$ | 1 | 0.968 | 109.9 | | | |
| 3 | 2 | 0.982 | 109.3 | 2.794 | −0.068 (2,2) | 167.6 |
| | 3 | 0.982 | 109.5 | 2.799 | | 166.6 |
| $(MeOH)_3$ | 1 | 0.983 | 110.1 | 2.776 | | 149.2 |
| (3) | 2 | 0.984 | 109.9 | 2.758 | | 151.2 |
| | 3 | 0.984 | 110.4 | 2.765 | | 150.7 |
| $(MeOH)_3$ | 1 | 0.971 | 109.0 | | | |
| 2 + 1 | 2 | 0.976 | 109.6 | 2.887 | 0.025 (2,2) | 167.0 |
| | 3 | 0.976 | 109.6 | 2.887 | 0.025 (2,2) | 167.0 |
| $(MeOH)_4$ | 1 | 0.969 | 109.8 | | | |
| 4 | 2 | 0.984 | 108.6 | 2.777 | −0.017 (3,2) | 175.6 |
| | 3 | 0.989 | 109.6 | 2.747 | −0.052 (3,3) | 171.1 |
| | 4 | 0.984 | 109.3 | 2.783 | | 169.5 |
| $(MeOH)_4$ | 1 | 0.990 | 109.7 | 2.737 | −0.029 ((3),avg) | 168.4 |
| (4) | 2 | 0.990 | 109.8 | 2.737 | −0.029 ((3),avg) | 168.4 |
| | 3 | 0.990 | 109.7 | 2.737 | −0.029 ((3),avg) | 168.4 |
| | 4 | 0.990 | 109.8 | 2.737 | −0.029 ((3),avg) | 168.4 |
| $(MeOH)_4$ | 1 | 0.970 | 109.2 | | | |
| $3 + 1_1$ | 2 | 0.980 | 109.6 | 2.834 | 0.040 (3,2) | 167.7 |
| | 3 | 0.981 | 109.6 | 2.808 | 0.009(3,3) | 165.0 |
| | 4 | 0.975 | 109.4 | 2.896 | 0.034 (2,2) | 167.6 |
| $(MeOH)_4$ | 1 | 0.964 | 110.0 | | | |
| $3 + 1_2$ | 2 | 0.985 | 109.6 | 2.761 | −0.033 (3,2) | 170.0 |
| | 3 | 0.979 | 109.4 | 2.843 | 0.044 (3,3) | 163.1 |
| | 4 | 0.978 | 109.1 | 2.854 | −0.008 (2,2) | 175.2 |
| $Me(OH)_4$ | 1 | 0.981 | 110.3 | 2.822 | 0.064 ((3),2) | 149.0 |
| (3) + 1 | 2 | 0.983 | 110.8 | 2.759 | −0.006 ((3),3) | 148.2 |
| | 3 | 0.987 | 109.7 | 2.737 | −0.039 ((3),1) | 152.4 |
| | 4 | 0.978 | 109.2 | 2.860 | −0.002 (2,2) | 172.6 |
| $(MeOH)_5$ | 1 | 0.992 | 109.5 | 2.718 | −0.019 ((4),avg) | 176.7 |
| (5) | 2 | 0.992 | 109.1 | 2.719 | −0.018 ((4),avg) | 175.9 |
| | 3 | 0.993 | 109.6 | 2.721 | −0.016 ((4),avg) | 177.9 |
| | 4 | 0.991 | 109.5 | 2.736 | −0.001 ((4),avg) | 175.4 |
| | 5 | 0.992 | 109.4 | 2.721 | −0.016 ((4),avg) | 177.5 |
| $(MeOH)_5$ | 1 | 0.984 | 109.5 | 2.809 | 0.072 ((4),avg) | 165.6 |
| (4) + 1 | 2 | 0.991 | 109.6 | 2.725 | −0.012 ((4),avg) | 167.4 |
| | 3 | 0.993 | 109.5 | 2.714 | −0.023 ((4),avg) | 168.5 |
| | 4 | 0.997 | 110.0 | 2.695 | −0.042 ((4),avg) | 170.6 |
| | 5 | 0.979 | 109.5 | 2.834 | −0.028 (2,2) | 168.5 |
| $(MeOH)_5$ | 1 | 0.980 | 110.0 | 2.823 | 0.065 ((3),2) | 147.1 |
| (3) + 2 | 2 | 0.984 | 110.5 | 2.750 | −0.015 ((3),3) | 149.1 |
| | 3 | 0.987 | 110.7 | 2.734 | −0.042 ((3),1) | 152.9 |
| | 4 | 0.984 | 109.5 | 2.775 | −0.019 (3,2) | 168.0 |
| | 5 | 0.982 | 109.4 | 2.801 | 0.002 (3,3) | 166.8 |
| $(MeOH)_5$ | 1 | 0.983 | 110.0 | 2.806 | −0.016 ((3)+1,1) | 149.5 |
| (3) + 1 + 1 | 2 | 0.979 | 109.5 | 2.849 | 0.090 ((3)+1,2) | 144.3 |
| | 3 | 0.989 | 110.1 | 2.729 | −0.008 ((3)+1,3) | 155.8 |
| | 4 | 0.978 | 109.6 | 2.809 | −0.051 ((3)+1,4) | 160.4 |
| | 5 | 0.979 | 109.6 | 2.820 | −0.040 ((3)+1,4) | 162.4 |

[a] Calculated at the Becke3LYP/6-31+G* level of theory. [b] Indices for the methanol units refer to labels from Figures 1−3. [c] Geometrical parameters are given for the respective methanol's interaction with the methanol to which it hydrogen donates. [d] $\Delta R_{OO}$ is the difference between the respective O-O distance and that for the HB in the structure to which it is to be compared. The compared structure is given in parentheses with its shortand notation and relevant MeOH unit identified. For the cyclic clusters, $\Delta R_{OO}$ is calculated relative to the average $R_{OO}$ of the indicated cyclic cluster.

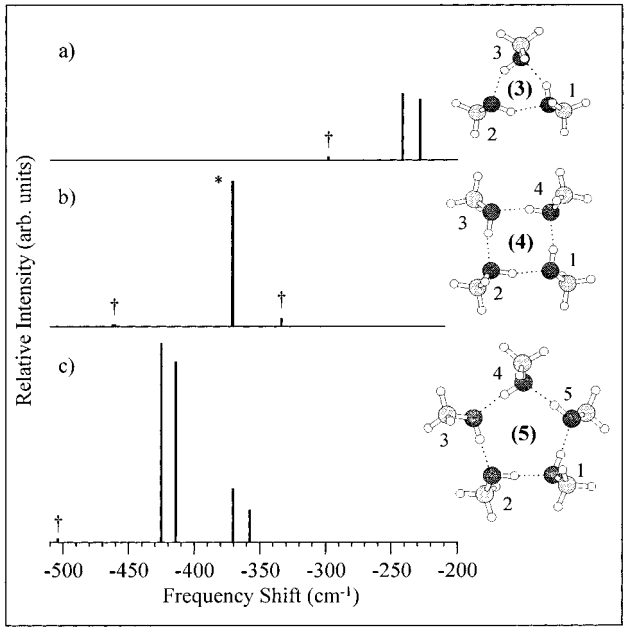


**Figure 1.** Stick diagram of the calculated OH stretch harmonic frequency shifts and infrared intensities for the cyclic methanol (a) trimer (3), (b) tetramer (4), and (c) pentamer (5). The frequency shift is relative to the OH stretch harmonic frequency for the methanol monomer at the same level of theory (3762.9 $cm^{-1}$). The structures giving rise to these spectra are shown as insets and are described in the text. The numbering of the methanol molecules corresponds with the numbering in Tables 1 and 4. The daggers (†) in the OH stretch spectra locate the positions of very weak transitions. In the cyclic tetramer spectrum, the transition marked with an asterisk is doubly degenerate with two unresolved transitions each of the indicated intensity.

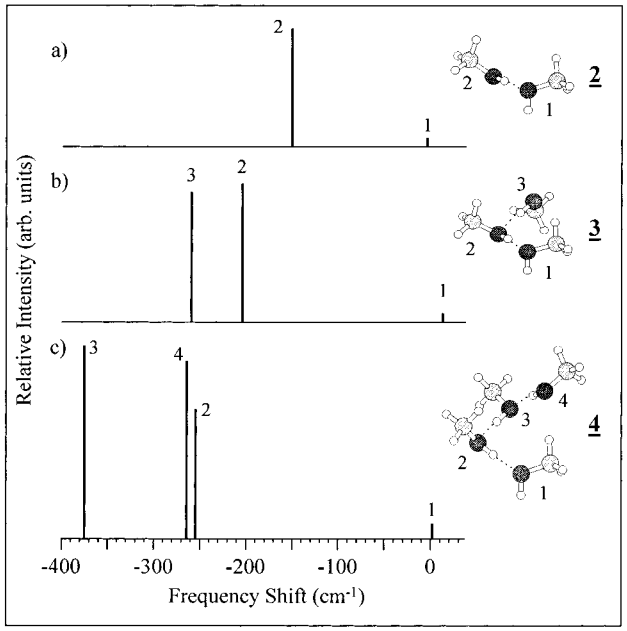


**Figure 2.** Stick diagram of the calculated OH stretch harmonic frequency shifts and infrared intensities for the chain methanol (a) dimer 2, (b) trimer 3, and (c) tetramer 4. The frequency shift is relative to the OH stretch harmonic frequency for the methanol monomer at the same level of theory (3762.9 $cm^{-1}$). The structures giving rise to these spectra are shown as insets and are described in the text. The numbering on the vibrational transitions corresponds to the methanol numbering in the inset and indicates which methanol OH has the largest coefficient-(s) in that normal mode (Table 4). See the text for further discussion.

The binding energy calculated for the dimer, after correction for ZPE and BSSE, is 3.70 kcal/mol with the 6-31+G* basis set and 3.43 kcal/mol with the 6-31+G′[2d,p] basis set, respectively. These values are in good agreement with the experimental value derived from infrared predissociation measurements ($D_0 = 3.2 \pm 0.1$ kcal/mol).[41]

The comparison of $R_{OO}$ and $D_0$ with the B3LYP/6-311++G-(2df,2p) calculations of Mo et al.[45] addresses the issue of convergence with increasing basis set size. The O−O separation for the dimer using B3LYP with the 6-31+G* and 6-31+G′-[2d,p] basis sets ($R_{OO} = 2.862$ and 2.881 Å, respectively) is virtually unchanged from the results using the much larger basis set (2.875 Å). The BSSE-corrected binding energies (−3.70/−3.43 kcal/mol) are in close agreement with experiment (−3.2 ± 0.1 kcal/mol) and also within 0.6 kcal/mol of the value (−3.08 kcal/mol) calculated with the G2(MP2/SVP) basis set,[45] which is specifically designed to determine accurate binding energies. Reasonable convergence is thereby demonstrated.

The MP2/VTZ(2df,2p) results of Bleiber and Sauer[42] on the methanol dimer provide a comparison of the B3LYP results against conventional, high-level ab initio methods. The MP2 O−O separation (2.831 Å) is 0.031 Å smaller than the B3LYP/6-31+G* result, but further from experiment (2.98 Å). The ZPE and BSSE-corrected binding energy of the MP2 calculation is −3.78 kcal/mol, very close to the B3LYP/6-31+G* result (−3.70 kcal/mol).

The OH stretch normal modes of the methanol dimer are nearly pure local mode donor and acceptor vibrations (Table 4), indicating that the OH−OH coupling across the hydrogen bond is small compared to the energy difference between (uncoupled) donor and acceptor levels. The experimental values[23] for the frequency shifts of donor and acceptor OH stretches of methanol dimer are +3 and −107 $cm^{-1}$. The Becke3LYP calculations give donor OH stretch frequency shifts

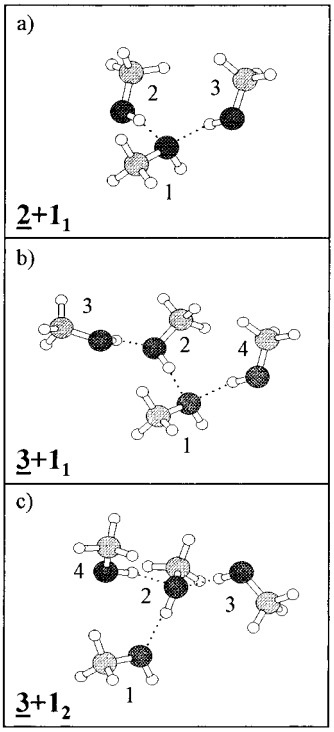


**Figure 3.** Calculated branched-chain structures for the methanol (a) trimer and (b), (c) tetramer. The structures are designated as $\underline{2} + 1_1$ and $\underline{3} + 1_1$, and $\underline{3} + 1_2$, respectively, where $\underline{n} + m_x$ denotes a chain of $n$ units long with a branch at molecule $x$ of chain length $m$ units attached. The numbering of the methanol molecules corresponds with the numbering in Tables 1 and 4.

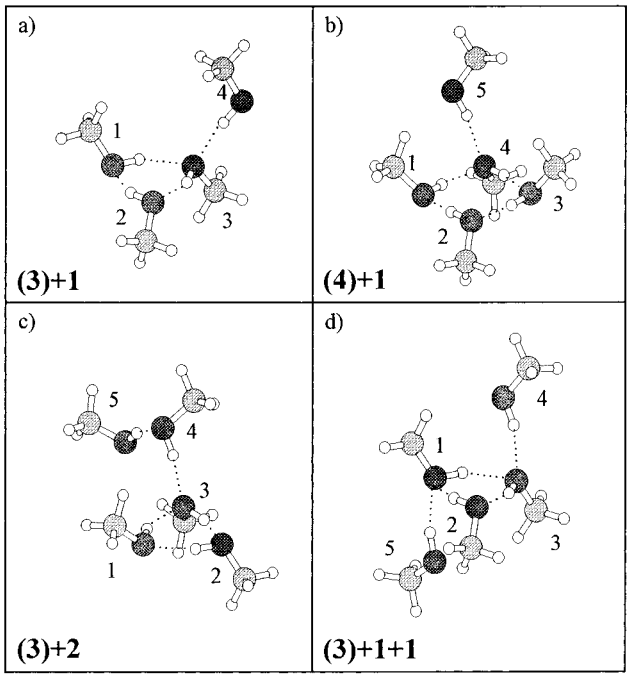


**Figure 4.** Calculated branched-cyclic structures for the methanol (a) (3) + 1 tetramer, (b) (4) + 1 pentamer, (c) (3) + 2 pentamer, and (d) (3)+1+1 pentamer. The structure designation (n) + *m* denotes an *n*-unit cycle with a branch of chain length *m* units attached. The numbering of the methanol molecules corresponds with the numbering in Tables 1 and 4.

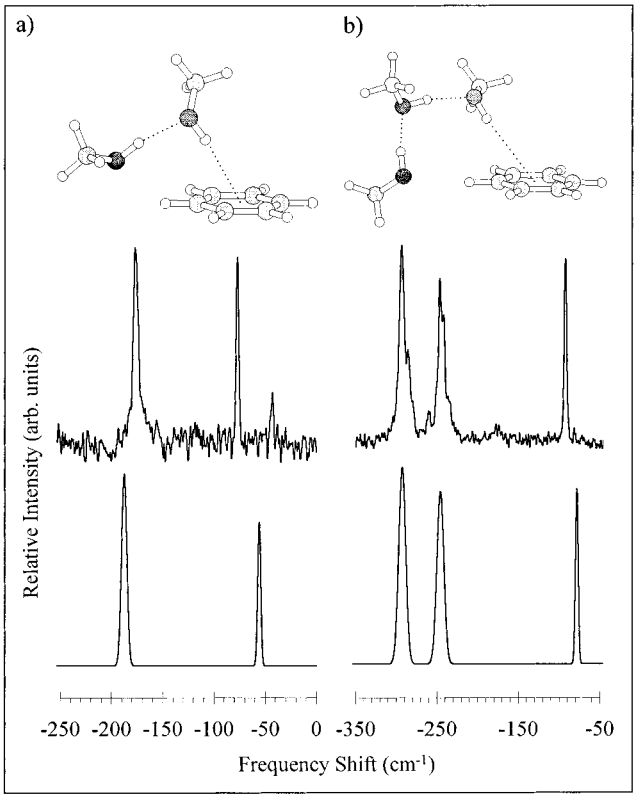


**Figure 5.** Calculated structure (top), experimental resonant ion-dip infrared spectrum in the OH stretch region (middle), and harmonic vibrational frequencies and infrared intensities calculated at the B3LYP/6-31+G* level of theory (bottom) for (a) benzene−(methanol)$_2$, and (b) benzene−(methanol)$_3$. The frequency shift of the experimental spectra is relative to the methanol monomer OH stretch fundamental (3681 cm$^{-1}$), while that for the calculation is the methanol monomer OH stretch harmonic frequency calculated at the same level of theory (3762.9 cm$^{-1}$).

which are somewhat too large (Table 6), with the results at the 6-31+G* basis set (−150.0 cm$^{-1}$) in better quantitative agreement with experiment. Calculations of the OH stretch frequency shifts using a variety of methods are included in Table 6 for comparison with the present work. It should be particularly noted that the present Becke3LYP frequency shifts using the 6-31+G* basis set are virtually identical with those using the much larger 6-311++G(3df,2p) from Mo et al. [45]

The analogous Becke3LYP 6-31+G* calculations on benzene−(methanol)$_2$ (bottom trace) are compared with experiment (upper trace) in Figure 5a. Besides the improved signal-to-noise, the new experimental data does not suffer from the decreased infrared power near 3500 cm$^{-1}$, which distorted the experimental intensities in our previous report.[36] In making the comparison, the calculated intensities have been convoluted over a Gaussian profile with width chosen to match the experimental widths. Note that the calculated frequency shifts of both donor (−187 cm$^{-1}$) and $\pi$ H-bonded OH (−56 cm$^{-1}$) stretches are in excellent agreement with the experimental values (−175 and −76 cm$^{-1}$, respectively). The calculated intensities also reproduce experiment satisfactorily.

**B. Cyclic Methanol Clusters.** *1. Structures and Binding Energies.* The lowest-energy structures for the cyclic methanol trimer (3), tetramer (4), and pentamer (5) are composed of planar ((3) and (4)) or nearly planar (5) OH···OH···O rings with methyl groups taking up alternating positions above and below the plane of the rings (Figure 1a−c). Each methanol molecule acts simultaneously as H-bond acceptor and donor (AD) to their nearest neighbors in the ring, thereby taking up nearly equivalent sites in the cluster. In the trimer[45] and pentamer, the odd number of methyl groups unavoidably juxtaposes two methyls on adjacent molecules, while the tetramer has $S_4$ symmetry. The asymmetry present in the trimer and pentamer leads to small differences in the O−O separations (Table 1). The O−O separations of the pentamer are also affected by the slight puckering of the ring (Figure 1c). Due to cooperative effects, the O−O separations in the cylic structures decrease with increasing ring size, approaching a limiting value near 2.72 Å in the pentamer. At the same time, the rather large nonlinearity of the H-bonds in the trimer (30°) and tetramer (12°) also approach asymptotic values near linear in the pentamer (∼4°).

The total (uncorrected) binding energies of the cyclic minimum-energy conformers for the trimer, tetramer, and pentamer are −18.4, −32.8 and −42.9 kcal/mol, respectively (Table 2). These are 3.5, 8.3, and 3.2 kcal/mol more stable, respectively, than the next most stable structures. The per H-bond binding energies are −6.1, −8.2, and −8.6 kcal/mol for the cyclic trimer, tetramer, and pentamer, respectively. The small increase in per H-bond binding between tetramer and pentamer follows the asymptotic approach to linear H-bonds in the larger cycles. The accompanying saturation in the cooperative strengthening of the H-bonds mirrors a similar effect calculated previously for cyclic water clusters.[64]

No experimental data is available on the O−O separation or binding energies of the cyclic methanol clusters. However, Mo et al. [45] have recently carried out both DFT and MP2 calculations on the cyclic methanol trimer using the 6-311+G(d,p) basis set. The O−O separations calculated by the MP2 and DFT methods are nearly identical (within 0.005 Å), despite the considerable time savings of the DFT calculation. The present B3LYP calculations using the 6-31+G* and 6-31+G′[2d,p] give O−O separations which straddle the 6-311+G(d,p) results but differ by less than 0.01 Å from them (Table 5). In the present DFT

**TABLE 2: Calculated Binding Energies for Methanol Cluster Conformers[a]**

| | binding energies | | | |
|---|---|---|---|---|
| structure | uncorrected | ZPE corrected[b] | ZPE[b] and BSSE corrected[c] | predicted[d] |
| $\underline{2}$ | −6.28 (−5.05) | −4.82 (−3.79) | −3.70 (−3.43) | |
| $\underline{3}$ | −14.94 (−12.28) | −11.88 (−9.58) | −9.58 | |
| (3) | −18.40 (−13.12) | −12.10 (−9.77) | −9.67 | |
| $\underline{2} + 1_1$ | −11.22 (−8.93) | −8.44 (−6.58) | −6.32 | 12.56 ($\underline{2} + \underline{2}$) − 1.3 = 11.26 |
| $\underline{4}$ | −24.02 | −19.33 | | |
| (4) | −32.82 | −27.19 | | |
| $\underline{3} + 1_1$ | −19.72 | −14.66 | | 21.22 ($\underline{3} + \underline{2}$) − 1.3 = 19.92 |
| $\underline{3} + 1_2$ | −21.08 | −16.75 | | 21.22 ($\underline{3} + \underline{2}$) = 21.22 |
| (3) + 1 | −24.53 | −20.02 | | 24.68 ((3) + $\underline{2}$) = 24.68 |
| (5) | −42.91 | −36.00 | | |
| (4) + 1 | −39.21 | −32.31 | | 39.10 ((4) + $\underline{2}$) = 39.10 |
| (3) + 2 | −33.78 | −26.89 | | 33.34 ((3) + $\underline{3}$) = 33.34 |
| (3) + 1 + 1 | −32.24 | −25.78 | | 30.96 ((3) + $\underline{2}$ + $\underline{2}$) = 30.96 |

[a] Values given were calculated at the Becke3LYP/6-31+G* level of theory while those in parentheses employed a 6-31+G′[2d,p] basis set. [b] These values are corrected for zero-point energy by frequency calculations at the prescribed level of theory. [c] These values are corrected for basis set superposition error by the full CP method at the prescribed level of theory. [d] Estimated binding energies of particular clusters, calculated using eqs 1 and 2 in the text.

study of the cyclic trimer, both ZPE and BSSE corrections have been made to the 6-31+G* results, leading to a best estimate of $D_0 = 9.67$ kcal/mol, just 0.09 kcal/mol more strongly bound that the methanol trimer chain (Table 2). The analogous B3LYP/6-311++G(3df,sp) value of Mo et al.[45] is 10.4 kcal/mol.

*2. OH Stretch Normal Modes, Vibrational Frequencies, and Infrared Intensities.* A schematic diagram of the OH stretch infrared spectra calculated for the cyclic trimer, tetramer, and pentamer are shown in parts a−c of Figure 1, respectively. All vibrational frequencies in the cyclic structures are far red-shifed from the monomer value (3763 $cm^{-1}$) because all the OH groups are involved in H-bonds of comparable strength. The average frequency shift of the vibrations increases in magnitude along the series (3), (4), and (5) (Figure 1a−c), consistent with the increased binding per H-bond in the larger rings.

The OH stretch normal modes are extensively delocalized over all OH bonds in the cycles, much as for the single donor vibrations in the cyclic water clusters.[64,66,77] The coupling of the OH groups in the ring breaks the near-degeneracy of the OH oscillators, leading to a range of vibrational frequencies which reflects the magnitude of the coupling. As pointed out by Honegger and Leutwyler for cyclic water clusters,[77] the OH stretch modes in the H-bonded ring can be thought of as longitudinal phonons with varying numbers of nodes in the phonon oscillation. In Table 4, the plus and minus signs indicate the relative phase of oscillation of the OH bond. In each case, the lowest frequency vibration is that with no nodes, while successively higher frequency modes have increasing numbers of nodes in its oscillation. Due to the symmetry of the OH groups in the cyclic structures, most of the OH stretch infrared intensity is carried by the near-degenerate pair of vibrations with two nodes (Table 4). The $S_4$ symmetry of the cyclic tetramer rigorously forbids the lowest frequency OH stretch mode, while the slightly asymmetric trimer and pentamer produce weak transitions in this mode.

The calculated frequency shifts for the OH stretch vibrations are in excellent agreement with recent gas-phase and matrix data on the cyclic trimer and the tentative experimental assignments of the cyclic tetramer OH stretch bands.[23,28,38,39] As Table 6 shows, the agreement is typically better than 20 $cm^{-1}$ for these cyclic clusters.

**C. Methanol Cluster Chains and Benzene−(Methanol)$_3$.** *1. Structures and Binding Energies.* The chain structures of the methanol trimer, $\underline{3}$, and tetramer, $\underline{4}$, are shown in parts b and c of Figure 2, respectively. In the chains, the methanol subunits have unique positions beginning with the acceptor methanol (A), followed by one or more acceptor/donor positions (AD) which are, in turn, capped by a single donor molecule (D). Despite the much less restrictive conditions on the H-bond linkage than in the cyclic clusters, the H-bonds in the chains are not strictly linear, but bend away from linear by 5−15° in adjusting to the small steric interactions and dispersive forces present in the cluster (Table 1). The signatures for stronger H-bonding (shorter $R_{OO}$ and longer $r_{OH}$) belong to the interior methanol molecules, though their values indicate somewhat weaker binding than in the cyclic structure of the same size. The effect of cooperativity in the chain is manifested in the decreasing O−O separation of the (terminal) donor methanol with the adjacent molecule. $R_{OO}$ shrinks from 2.862 to 2.799 to 2.783 Å as the chain size increases from dimer to trimer to tetramer, respectively. Not surprisingly, the majority of the decrease occurs in going from the dimer to the trimer chain, as would occur if the effects of lengthening the chain primarily influence a given molecule's nearest neighbors in the chain.

The binding energies of the chain trimer (14.94 kcal/mol) and tetramer (24.02 kcal/mol) are 3.5 and 8.3 kcal/mol smaller in magnitude than their cyclic counterparts. Including ZPE corrections, these differences are 2.8 and 7.7 kcal/mol, indicating a clear energetic preference for formation of cyclic over chain structures in these small clusters. The average H-bond energy calculated for the trimer chain (7.47 kcal/mol) is significantly greater than in the cyclic trimer (6.13 kcal/mol), but this is more than compensated by the extra H-bond in the cyclic structure. In the chain tetramer, even the average energy per H-bond (8.01 kcal/mol) is smaller than in the cyclic structure (8.21 kcal/mol). This is a consequence of the smaller cooperativity in the chain structures.

As reported in our previous publication,[36] the experimentally observed benzene−(methanol)$_3$ cluster incorporates the methanol trimer as a H-bonded chain rather than a cycle. The implication is that, in the presence of the "solute" benzene, the lowest-energy structure for the "solvent" methanol trimer is changed from a cycle to a chain. The B3LYP/6-31+G* calculations correctly predict this reversal (albeit in the absence of ZPE and BSSE corrections), with the benzene−(methanol trimer chain) (hereafter Bz-$\underline{3}$) over 5 kcal/mol more stable than Bz-(3) (Table 2). The lesser number of methanol-methanol H-bonds in Bz-$\underline{3}$ than Bz-(3) is in this case more than compensated by (i) the greater strength of the H-bonds in the trimer chain over the cycle and (ii) the much stronger attraction of the chain for benzene. As Figure 5b) shows, the trimer chain is of a length that enables

**TABLE 3: Calculated Vibrational Quantities for Methanol Cluster Conformers**[a]

| | frequency (in $cm^{-1}$) | frequency shift[b] (in $cm^{-1}$) | intensity (in km/mol) |
|---|---|---|---|
| $(MeOH)_1$ | 3762.9 | 0.0 | 24.1 |
| $(MeOH)_2$ | 3612.9 | −150.0 | 516.9 |
| 2 | 3758.6 | −4.3 | 38.5 |
| $(MeOH)_3$ | 3503.8 | −259.1 | 607.7 |
| 3 | 3559.4 | −203.5 | 649.6 |
| | 3776.3 | 13.4 | 37.2 |
| $(MeOH)_3$ | 3465.2 | −297.7 | 30.1 |
| (3) | 3521.4 | −241.5 | 853.8 |
| | 3534.9 | −228.0 | 778.4 |
| $(MeOH)_3$ | 3635.9 | −127.0 | 599.7 |
| $2 + 1_1$ | 3654.5 | −108.4 | 260.7 |
| | 3746.8 | −16.1 | 50.3 |
| $(MeOH)_4$ | 3388.3 | −374.6 | 903.9 |
| 4 | 3499.2 | −263.7 | 831.8 |
| | 3508.3 | −254.6 | 603.5 |
| | 3764.8 | 1.9 | 38.8 |
| $(MeOH)_4$ | 3301.1 | −461.8 | 0.0 |
| (4) | 3392.0 | −370.9 | 1861.7 |
| | 3392.3 | −370.6 | 1867.1 |
| | 3429.3 | −333.6 | 93.3 |
| $(MeOH)_4$ | 3521.4 | −241.5 | 559.8 |
| $3 + 1_1$ | 3575.9 | −187.0 | 588.4 |
| | 3651.4 | −111.5 | 373.2 |
| | 3752.5 | −10.4 | 49.8 |
| $(MeOH)_4$ | 3485.2 | −277.7 | 752.9 |
| $3 + 1_2$ | 3582.9 | −180.0 | 644.7 |
| | 3617.0 | −145.9 | 379.4 |
| | 3771.7 | 8.8 | 40.4 |
| $(MeOH)_4$ | 3436.3 | −326.6 | 413.9 |
| $(3) + 1$ | 3520.4 | −242.5 | 656.6 |
| | 3559.4 | −203.5 | 711.6 |
| | 3604.0 | −158.9 | 426.2 |
| $(MeOH)_5$ | 3259.0 | −503.9 | 42.6 |
| (5) | 3338.0 | −424.9 | 2557.2 |
| | 3348.8 | −414.1 | 2309.5 |
| | 3392.5 | −370.4 | 297.9 |
| | 3405.2 | −357.7 | 178.2 |
| $(MeOH)_5$ | 3231.0 | −531.9 | 641.9 |
| $(4) + 1$ | 3333.0 | −429.9 | 1447.6 |
| | 3386.9 | −376.0 | 1095.0 |
| | 3506.9 | −256.0 | 617.7 |
| | 3597.0 | −165.9 | 521.2 |
| $(MeOH)_5$ | 3432.3 | −330.6 | 644.1 |
| $(3) + 2$ | 3486.9 | −276.0 | 734.8 |
| | 3511.0 | −251.9 | 435.4 |
| | 3534.8 | −228.1 | 752.0 |
| | 3580.5 | −182.4 | 540.8 |
| $(MeOH)_5$ | 3399.3 | −363.6 | 590.2 |
| $(3) + 1 + 1$ | 3529.5 | −233.4 | 613.3 |
| | 3576.5 | −186.4 | 296.2 |
| | 3609.5 | −153.4 | 113.4 |
| | 3617.7 | −145.2 | 887.2 |

[a] Calculated at the Becke3LYP/6-31+G* level of theory. [b] Relative to the methanol monomer O−H stretch at the same level of theory.

it to bind appreciably both to benzene's $\pi$ cloud as a H-bond donor and to the aryl C−H as a (weak) H-bond acceptor. The effect of benzene on the terminal OH which forms the $\pi$ H-bond is best seen in the increase in its $r_{OH}$ from 0.968 Å in 3 to 0.975 Å in Bz-3.

*2. OH Stretch Normal Modes, Vibrational Frequencies, and Intensities.* Figure 2b,c presents the calculated OH stretch infrared spectra of the methanol trimer and tetramer chains. A spectroscopic signature of the chain structures is the free OH stretch fundamental (near zero frequency shift), which is notably absent from the calculated spectra of either the cyclic or branched-cyclic structures. The free OH stretch is quite weak and is relatively unchanged in either frequency or intensity from its value in the methanol dimer as the chain length grows. The other OH stretch modes all carry appreciable intensity in the chain structures due to their lack of symmetry by comparison to the cyclic clusters.

As Table 4 shows, the normal modes in the chain clusters are quite highly localized on single OH bonds. In all the modes of 3 and 4, this localization is greater than 80%, reflecting the unique H-bonding environment of each methanol in the chain.

Given the significant localization of the normal modes, the vibrational frequencies of Table 3 are strongly correlated with the key structural parameters of the H-bond in which they are involved (Table 1). A longer $r_{OH}$, more nearly linear H-bond, and shorter $R_{OO}$ give rise to a lower OH stretch vibrational frequency (larger frequency shift).

The only OH stretch infrared data on the pure methanol chain clusters is the matrix data on the trimer chain from the elegant work of Coussan et al.[38,39] Once again, the calculated frequency shifts in Table 3 (+13, −203, and −259 $cm^{-1}$) are in good quantitative agreement with the experimental frequency shifts of the three OH stretch bands of −2, −231, and −274 $cm^{-1}$ (relative to the methanol monomer OH stretch of 3664 $cm^{-1}$ in the matrix.

The calculated OH stretch IR spectrum for Bz-3 is compared with our newly acquired resonant ion-dip infrared spectrum in Figure 5b. Again, the calculated frequency shifts (−292, −246, −78 $cm^{-1}$) are in excellent agreement with experiment (−292, −246, −92 $cm^{-1}$), differing appreciably only in the $\pi$ H-bonded OH stretch, whose frequency shift is somewhat underestimated. The cooperative strengthening of the $\pi$ H-bond to benzene with increasing methanol chain length is evidenced by the increasing OH stretch frequency shift calculated along the $BM_{1-3}$ series (−33, −57, and −78 $cm^{-1}$, respectively).

**D. Branched Methanol Chains.** *1. Structures and Binding Energies.* Three small branched-chain structures have been investigated, the $2 + 1_1$ trimer (Figure 3a), the $3 + 1_1$ tetramer (Figure 3b), and the $3 + 1_2$ tetramer (Figure 3c). The $2 + 1_1$ structure is one in which one methanol acts as double acceptor (AA, molecule 1) to two other methanols. This structure has also been identified as a local minimum in the recent calculations by Mo et al.[45] The optimized structure for this cluster retains $C_s$ symmetry, with the two donor molecules taking up equivalent H-bonding positions relative to the two lone pairs on the double-acceptor oxygen. This structure can be viewed as two dimer segments sharing the same acceptor methanol. The presence of two hydrogen bonds to the same methanol leads to an increase of 0.025 Å in the O−O separation of the two H− bonds relative to the dimer. At the same time, the steric hindrance associated with formation of a double-acceptor methanol also increases the nonlinearity of the hydrogen bonds from 6° in the dimer to 13° in the $2 + 1_1$ structure.

The $3 + 1_1$ and $3 + 1_2$ tetramer structures probe the effects of a branch on the trimer chain. Relative to one another, the two structures test the effects of the position of the branch point on the chain. As Table 1 shows, the O−O separation of the H-bond from methanol 4 to methanol 3 (hereafter designated as the 4→3 hydrogen bond) is very similar (2.896 and 2.854 Å) in the $3 + 1_1$ and $3 + 1_2$ structures, indicating that the point of attachment is not of great consequence to the H-bond strength of the branch. In the $3 + 1_1$ structure (Figure 3b), the attachment of the monomer branch to the trimer chain lengthens the original H-bond 2→1 by $\Delta R_{OO} = +0.040$ Å but has a relatively modest effect (+0.009 Å) on the 3→2 H-bond which is once removed from the branch point. Similar effects are seen

**TABLE 4: Projection of the O−H Stretch Normal Modes onto the MeOH Unit OH Bonds[a]**

| | MeOH unit[b] | O−H stretch normal modes[c] | | | | |
|---|---|---|---|---|---|---|
| | | $\nu_5$ | $\nu_4$ | $\nu_3$ | $\nu_2$ | $\nu_1$ |
| $(MeOH)_2$ | 1 | | | | (+) 0.001 | (−) 0.999 |
| 2 | 2 | | | | (+) 0.999 | (+) 0.001 |
| $(MeOH)_3$ | 1 | | | (−) 0.000 | (−) 0.000 | (+) 1.000 |
| 3 | 2 | | | (+) 0.172 | (−) 0.827 | (−) 0.000 |
| | 3 | | | (+) 0.828 | (+) 0.173 | (−) 0.000 |
| $(MeOH)_3$ | 1 | | | (+) 0.198 | (−) 0.011 | (−) 0.793 |
| (3) | 2 | | | (+) 0.371 | (−) 0.471 | (+) 0.149 |
| | 3 | | | (+) 0.431 | (+) 0.518 | (+) 0.058 |
| $(MeOH)_3$ | 1 | | | (−) 0.000 | (+) 0.006 | (+) 0.995 |
| $2 + 1_1$ | 2 | | | (−) 0.500 | (+) 0.497 | (−) 0.003 |
| | 3 | | | (+) 0.500 | (+) 0.497 | (−) 0.003 |
| $(MeOH)_4$ | 1 | | (−) 0.000 | (−) 0.000 | (+) 0.000 | (+) 1.000 |
| 4 | 2 | | (+) 0.053 | (+) 0.017 | (+) 0.930 | (−) 0.000 |
| | 3 | | (+) 0.886 | (+) 0.051 | (−) 0.065 | (−) 0.000 |
| | 4 | | (+) 0.062 | (−) 0.933 | (+) 0.004 | (−) 0.000 |
| $(MeOH)_4$ | 1 | | (+) 0.250 | (+) 0.254 | (−) 0.246 | (−) 0.252 |
| (4) | 2 | | (+) 0.250 | (−) 0.246 | (−) 0.254 | (+) 0.252 |
| | 3 | | (+) 0.250 | (−) 0.254 | (+) 0.246 | (−) 0.252 |
| | 4 | | (+) 0.250 | (+) 0.246 | (+) 0.254 | (+) 0.244 |
| $(MeOH)_4$ | 1 | | (+) 0.000 | (−) 0.001 | (−) 0.003 | (−) 0.996 |
| $3 + 1_1$ | 2 | | (+) 0.149 | (−) 0.837 | (−) 0.019 | (+) 0.001 |
| | 3 | | (+) 0.849 | (+) 0.144 | (+) 0.000 | (−) 0.000 |
| | 4 | | (−) 0.002 | (+) 0.018 | (−) 0.978 | (+) 0.003 |
| $(MeOH)_4$ | 1 | | (+) 0.000 | (−) 0.000 | (−) 0.000 | (−) 0.999 |
| $3 + 1_2$ | 2 | | (+) 0.952 | (−) 0.007 | (+) 0.040 | (+) 0.001 |
| | 3 | | (+) 0.032 | (+) 0.691 | (−) 0.273 | (−) 0.000 |
| | 4 | | (+) 0.016 | (−) 0.302 | (−) 0.687 | (−) 0.001 |
| $(MeOH)_4$ | 1 | | (+) 0.038 | (−) 0.082 | (−) 0.801 | (+) 0.077 |
| (3) + 1 | 2 | | (+) 0.080 | (−) 0.805 | (+) 0.114 | (−) 0.001 |
| | 3 | | (+) 0.871 | (+) 0.101 | (+) 0.003 | (−) 0.020 |
| | 4 | | (+) 0.010 | (+) 0.012 | (+) 0.082 | (+) 0.902 |
| $(MeOH)_5$ | 1 | (+) 0.238 | (+) 0.214 | (+) 0.190 | (−) 0.315 | (−) 0.035 |
| (5) | 2 | (+) 0.242 | (−) 0.088 | (+) 0.293 | (+) 0.380 | (−) 0.002 |
| | 3 | (+) 0.219 | (−) 0.415 | (−) 0.063 | (−) 0.183 | (+) 0.113 |
| | 4 | (+) 0.119 | (−) 0.001 | (−) 0.281 | (+) 0.018 | (−) 0.590 |
| | 5 | (+) 0.182 | (+) 0.282 | (−) 0.172 | (+) 0.103 | (+) 0.260 |
| $(MeOH)_5$ | 1 | (+) 0.002 | (+) 0.001 | (+) 0.000 | (−) 0.048 | (−) 0.952 |
| (4) + 1 | 2 | (+) 0.052 | (−) 0.261 | (−) 0.649 | (−) 0.030 | (+) 0.000 |
| | 3 | (+) 0.185 | (−) 0.490 | (+) 0.326 | (−) 0.000 | (+) 0.000 |
| | 4 | (+) 0.740 | (+) 0.246 | (−) 0.002 | (−) 0.007 | (+) 0.006 |
| | 5 | (+) 0.021 | (−) 0.002 | (−) 0.023 | (+) 0.915 | (−) 0.042 |
| $(MeOH)_5$ | 1 | (+) 0.022 | (−) 0.042 | (+) 0.007 | (+) 0.031 | (−) 0.898 |
| (3) + 2 | 2 | (+) 0.110 | (−) 0.091 | (+) 0.743 | (−) 0.023 | (+) 0.029 |
| | 3 | (+) 0.798 | (−) 0.015 | (−) 0.154 | (+) 0.015 | (+) 0.023 |
| | 4 | (+) 0.064 | (+) 0.561 | (+) 0.013 | (−) 0.318 | (−) 0.046 |
| | 5 | (+) 0.006 | (+) 0.290 | (+) 0.084 | (+) 0.613 | (+) 0.003 |
| $(MeOH)_5$ | 1 | (+) 0.035 | (−) 0.848 | (−) 0.035 | (+) 0.000 | (−) 0.079 |
| (3) + 1 + 1 | 2 | (+) 0.012 | (−) 0.010 | (−) 0.163 | (+) 0.395 | (+) 0.416 |
| | 3 | (+) 0.949 | (+) 0.032 | (+) 0.003 | (−) 0.015 | (+) 0.000 |
| | 4 | (+)0.004 | (+) 0.040 | (+) 0.009 | (+) 0.543 | (−) 0.405 |
| | 5 | (+) 0.000 | (−) 0.071 | (+) 0.790 | (+) 0.047 | (+) 0.099 |

[a] Normal modes based on the Becke3LYP/6-31+G* level of theory. [b] Indices for the methanol units refer to labels from Figures 1−4. [c] Relative phases of the O−H stretches are given in parentheses.

in the $\underline{3} + 1_2$ structure, but in this case it is the 3→2 hydrogen bond which is lengthened (by 0.044 Å), since molecule 2 is now the attachment point for the branch. Here, a counteracting contraction (−0.033 Å) is seen in the O−O separation of the 2→1 H-bond, suggesting that the formation of a double-acceptor methanol at the branch point strengthens the donating H-bond of the double acceptor molecule with its neighbor. Similar trends are seen in the OH bond lengths: $r_{OH}(3)$ in $\underline{3} + 1_2$ is shortened by 0.003 Å from its value in $\underline{3}$, while $r_{OH}(2)$ is lengthed by 0.003 Å.

We will see that these two counteracting effects are general results of the attachment of a branch to either a chain or cycle; namely, that the formation of the "branch" H-bond weakens the H-bond on the other branch of the "Y" and strengthens the H-bond to the stem of the Y, as shown schematically below:

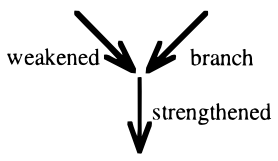


Put another way, an AAD methanol has weaker acceptor H-bonds than an AD molecule but a stronger donor H-bond. A similar conclusion was reached recently by Mo et al. in their studies of water trimers.[80]

**TABLE 5: Comparison of the Calculated and Experimental Binding Energies and Selected Structural Parameters for Various Sized Methanol Clusters**

| | | exptl | Becke3LYP/ 6-31+G* w/ZPE[a] | Becke3LYP/ 6-31+G′[2d,p] w/ZPE[a] | MP2/ 6-31+G* and w/ZPE[a] | HF/ 6-311++G (2d,2p) w/ZPE and BSSE[b] | B3LYP/ 6-311++G(3df,2p) and G2(MP2,SVP) w/ZPE | MP2/VTZ (2df,2p) w/ZPE and BSSE[b] | MP2/ ESPB w/ZPE[a] | OPLS[c] | PHH3[c] |
|---|---|---|---|---|---|---|---|---|---|---|---|
| reference | | | this work | this work | this work | 37 | 45 | 42 | 40 | 53 | 53 |
| $(MeOH)_2$ $\underline{2}$ | B.E. (kcal/mol) | $-3.2 \pm 0.1$[d] | −4.82/−3.70[b] | −3.79/−3.43[b] | −7.73/−6.08 | −4.12 | −3.55/−3.08 | −3.78 | −3.5 | −6.8 | −5.60 |
| | $r_{OH,acceptor}$ (Å) | | 0.969 | 0.963 | 0.974 | 0.938 | 0.962 | | | | |
| | $r_{OH,donor}$ (Å) | | 0.977 | 0.972 | 0.980 | 0.942 | 0.970 | | | | |
| | $R_{oo}$ (Å) | 2.98(2)[e] | 2.862 | 2.81 | 2.861 | 3.011 | 2.875 | 2.831 | 2.96 | 2.74 | 2.85 |
| | $a_{OHO}$ (deg) | | 174.2 | 174.1 | 175.8 | 176.9 | 177.4 | 172.2 | | | |
| $(MeOH)_3$ (3) | B.E. (kcal/mol) | | −14.65/−12.23[b] | −11.97 | | −11.95 | −11.52/−10.20 | | | −17.55 | −14.14 |
| | avg. $r_{OH}$ (Å) | | 0.984 | 0.977 | | 0.944 | 0.976 | | | | |
| | avg. $R_{oo}$ (Å) | | 2.766 | 2.787 | | 2.932 | 2.771 | | | | |
| | $a_{OHO}$ (deg) | | 150.4 | 151.9 | | 149.6 | 149.0 | | | | |
| $(MeOH)_4$ (4) | B.E. (kcal/mol) | | −27.19 | | | | | | | −29.82 | −23.51 |
| | avg. $R_{oo}$(Å) | | 2.737 | | | | | | | | |
| | $a_{OHO}$ (deg) | | 168.4 | | | | | | | | |
| $(MeOH)_5$ (5) | B.E. (kcal/mol) | | −36.00 | | | | | | | −39.72 | −31.65 |
| | avg. $R_{oo}$ (Å) | | 2.723 | | | | | | | | |
| | $a_{OHO}$ (deg) | | 176.7 | | | | | | | | |

[a] The binding energies are corrected for ZPE. [b] The binding energies are corrected for both ZPE and BSSE. [c] The binding energies are not corrected for ZPE or BSSE. [d] Reference 41. [e] Reference 27.

The binding energies listed in Table 2 clearly predict a strong discrimination against branched-chain structures on energetic grounds. In the $\underline{2} + 1_1$ structure, the binding energy (Table 2) before ZPE correction is only −11.22 kcal/mol, about 1.3 kcal/mol smaller in magnitude than that of two independent methanol dimer H-bonds (−12.56 kcal/mol). This reflects the weakened H-bonds associated with formation of the double-acceptor methanol molecule.

The uncorrected binding energy for the $\underline{3} + 1_1$ structure is only 19.7 kcal/mol, over 13 kcal/mol smaller than the most strongly bound tetramer structure, the cyclic tetramer (4). The $\underline{3} + 1_1$ structure has several energetic liabilities: (i) it possesses one fewer hydrogen bond than the cyclic tetramer, (ii) the magnitude of the cooperative effects in the chain is smaller than in cyclic structures, and (iii) the two "branch-point" hydrogen bonds are weaker than their unbranched analogues. Energetically, formation of an AAD molecule in the $\underline{3} + 1_2$ structure leads to largely compensating effects; that is, the stem H-bond is strengthened by an amount roughly equal to the weakening in the two branch H-bonds. On the other hand, when the branch forms a double-acceptor methanol (such as in $\underline{2} + 1$ and $\underline{3} + 1_1$), the weakening of the branch H-bonds is not compensated by the stronger AAD donor H-bond, thereby decreasing the net binding over the sub-structure sum by about 1.3 kcal/mol (Table 2). Thus an approximate binding energy for the $\underline{2} + 1$, $\underline{3} + 1_1$, and $\underline{3} + 1_2$ structures can be obtained from

$$\mathrm{BE}[\underline{\mathrm{n}}+\mathrm{b}] \approx \mathrm{BE}[\underline{\mathrm{n}}] + \mathrm{BE}[\underline{\mathrm{b}+1}] - 1.3(\#\mathrm{AA}) \qquad (1)$$

where "n" is the length of the longest chain, "b" is the length of the branch, and "#AA" is the number of double-acceptor methanols in the structure.

*2. OH Stretch Normal Modes, Vibrational Frequencies, and Intensities.* Given the structural and energetic consequences of branch formation one can readily anticipate the effects of branch formation on the OH stretch vibrational frequencies and intensities.

(1) The branched chains retain a free OH stretch.

(2) Since the OH stretch modes of the chain structures are already nearly local mode in character, the attachment of the branch largely retains this localization.

(3) The OH stretch mode associated with the single-molecule branch is just to the high-frequency side of the donor OH stretch of a methanol dimer due to the weakened H-bond associated with branch formation.

(4) The more symmetric structures ($\underline{2} + 1$ and $\underline{3} + 1_2$) have some delocalization of the OH stretch modes of the equal length branches (Table 4). This coupling splits the two terminal donor OH stretch levels.

(5) The OH stretch frequency of the strengthened AAD H-bond in the $\underline{3} + 1_2$ structure is shifted down in frequency by 74 $cm^{-1}$ from its value in the unbranched trimer chain.

The only experimental data on the branched-chain structures is that tentatively assigned to the $\underline{3} + 1_1$ structure by Coussan et al. in a $N_2$ matrix.[39] Bands with frequency shifts of −18, −195, −233, and −281 $cm^{-1}$ are assigned to this structure based on the changes expected upon breaking a H-bond in a (3) + 1 branched cycle. The correspondence with our computed frequencies (−10, −111, −187, −241 $cm^{-1}$) is not as good as might be expected on the basis of their close proximity for other structures. Whether matrix effects, incorrect assignment, or deficiencies in the calculation are responsible for these differences is not known.

**TABLE 6: Comparison of the Calculated and Experimental OH and CO Vibrational Frequency Shifts[a] for Various Sized Methanol Clusters**

| | | exptl | Becke-3LYP/6-31+G* | Becke3LYP/6-31+G′[2d,p] | HF/6-311++G(2d,2p) | Becke3LYP/6-311++G(3df,2p) | MP2/DZP | MP2/ESPB | OPLS | PHH3 |
|---|---|---|---|---|---|---|---|---|---|---|
| | reference | | this work | this work | 37 | 45 | 42 | 40 | 53 | 53 |
| $(MeOH)_2$ | $\nu_1$ | $+2.6^b/+1^c$ | −4.3 | −14.8 | −5 | −3 | | | +20.6 | +70.3 |
| 2 | $\nu_2$ | $-107.1^b/-107^c$ | −150.0 | −188.2 | −69 | −148 | −131 | −126 | −239.4 | −145.1 |
| | CO stretch | $+18^c$ | +17.4 | +20.1 | +10 | | | | +28.9 | +24.2 |
| | | $-7^c$ | −13 | −12.5 | −14 | | | | +1.3 | −1.7 |
| $(MeOH)_3$ | $\nu_1$ | $-2^d$ | 13.4 | 2.7 | | | | | | |
| 3 | $\nu_2$ | $-231^d$ | −203.5 | −254.7 | | | | | | |
| | $\nu_3$ | $-275^d$ | −259.1 | −303.5 | | | | | | |
| $(MeOH)_3$ | $\nu_1$ | $-178^e$ | −228.0 | −255.4 | −98 | −234 | | | | |
| (3) | $\nu_2$ | $-219^b/-209^e$ | −241.5 | −274.7 | −103 | −246 | | | | |
| | $\nu_3$ | $-247^e$ | −297.7 | −329.1 | −128 | −300 | | | | |
| | CO stretch | $+8^c$ | +7.7 | +9.2 | +0. | | | | +3.8 | +64.3 |
| $(MeOH)_4$ | $\nu_{2,3}$ | $-380^d$ | −370.6, −370.9 | | | | | | | |
| (4) | CO stretch | $+10^c$ | +12.1 | | | | | | +24.9 | +26.6 |
| $(MeOH)_4$ | $\nu_1$ | $-162^f$ | −158.9 | | | | | | | |
| (3) + 1 | $\nu_2$ | | −203.5 | | | | | | | |
| | $\nu_3$ | $-239^f$ | −242.5 | | | | | | | |
| | $\nu_4$ | $-294^f$ | −326.6 | | | | | | | |
| $(MeOH)_4$ | $\nu_1$ | $-18^f$ | −10.4 | | | | | | | |
| $3 + 1_1$ | $\nu_2$ | $-195^f$ | −111.5 | | | | | | | |
| | $\nu_3$ | $-233^f$ | −187.0 | | | | | | | |
| | $\nu_4$ | $-281^f$ | −241.5 | | | | | | | |
| $(MeOH)_5$ | CO stretch | | +7.5 | | | | | | +27.5 | +16.9 |
| (5) | | $+14^c$ | +13.4 | | | | | | +21.0 | +16.6 |
| | | | +17.1 | | | | | | +17.2 | +14.7 |
| Bz−$(MeOH)_2$ | $\nu_1$ | $-76^g$ | −55.6 | | | | | | | |
| Bz-2 | $\nu_2$ | $-175^g$ | −187.4 | | | | | | | |
| Bz−$(MeOH)_3$ | $\nu_1$ | $-92^g$ | −77.9 | | | | | | | |
| Bz- 3 | $\nu_2$ | $-246^g$ | −245.6 | | | | | | | |
| | $\nu_3$ | $-292^g$ | −292.5 | | | | | | | |

[a] Frequency shifts are calculated relative to the frequency of the OH stretch in the free monomer at the same level of theory. All values are in $cm^{-1}$. [b] Reference 23. [c] Reference 5. [d] From infrared spectroscopy of matrix-isolated methanol clusters by Coussan *et al*. (refs 38, 39). [e] Reference 8. [f] Reference 39. Note that experimental values for structure $3 + 1_1$ are from a tentative assignment. [g] Reference 36.

**E. Branched Methanol Cycles.** *1. Structures and Binding Energies.* Four branched-cycle structures have been studied: the (3) + 1 tetramer (Figure 4a), the (4) + 1 pentamer (Figure 4b), the (3) + 2 pentamer (Figure 4c), and the (3) + 1 + 1 double-branched pentamer (Figure 4d). The addition of a branch to a cyclic structure has similar structural consequences (Table 1) to those just noted in the H-bonded chain; namely, weakening of the double-acceptor H-bonds and strengthening of the AAD donor H-bond.

In the (3) + 1 structure, the monomer branch has three nearly-equivalent attachment points to (3) via the unoccupied lone pairs on the methanol oxygens. At the present level of theory, the structure in Figure 4a is 0.2 kcal/mol more strongly bound than the alternate one in which the branch attaches to molecule 1 on the opposite face of the cycle. Vibrational frequencies have been calculated only for the former structure.

While the hydrogen bonding and methyl group orientations of the cyclic trimer are retained upon addition of the branch, the cycle is significantly distorted in (3) + 1 from the near-symmetric structure it has in (3). Once again, the most dramatic effects involve the two hydrogen bonds in the cycle at the AAD "branch point" (molecule 3, Figure 4a), shortening the donor hydrogen bond (from molecule 3→2 in Figure 4a) by 0.039 Å from its value in the cyclic trimer, but lengthening the 1→3 hydrogen bond by an even greater amount (0.064 Å). The O−O separation in the branch H-bond is very close to its value in the methanol dimer.

Not surprisingly, in the (4) + 1 structure (Figure 4b), similar distortions due to branch formation are evident (Table 1).

The (3) + 2 structure (Figure 4c) tests the effects of extending the length of the branch to a dimer unit. One sees that the O−O separations in the trimer cycle (Table 1) are hardly changed from what was already induced by the monomer branch in the (3) + 1 structure. Furthermore, the dimer branch itself is structurally very similar to the last two members of a trimer chain (Table 4).

The (3)+1+1 structure (Figure 4d, Table 1) probes the addition of a second monomer branch to the (3) + 1 structure. In Table 1, the change in O−O separation ($\Delta R_{OO}$) is given relative to the (3) + 1 structure. The largest structural changes induced by the second branch are the shortening of both branch O−O separations (by −0.051 and −0.040 Å). This suggests some cooperative strengthening of the branches when adjacent to one another. As expected, the addition of the second branch (molecule 5) also lengthens the 2→1 O−O separation. The shortening of the AAD H-bond (1→3) when a second branch is added is only 0.016 Å because this H-bond is already constrained to be a double-acceptor H-bond by the presence of the first branch.

As with the branched chain clusters, the calculated binding energies of the branched cycles (uncorrected for ZPE and BSSE) are closely reproduced by a simple sum of contributions from the relevant sub-structures using

$$\mathrm{BE}\,[(n)+\underline{b}] \approx \mathrm{BE}[(n)] + \mathrm{BE}[\underline{b+1}] \qquad (2)$$

where "n" is now the number of methanols in the cycle. Equation 2 produces binding energies within a few tenths of a kcal/mol of the calculations on the "full" cluster for all cases

but the double-branch structure. In addition, the change in total binding energy upon addition of a single-molecule branch is almost the same (∼6.1 kcal/mol at the present level of theory) regardless of the type of structure (cycle/chain) or size of the cluster (cyclic trimer or tetramer).

*2. OH Stretch Normal Modes, Vibrational Frequencies, and Intensities.* In the (3) + 1 structure, the normal modes (Table 4) are largely localized in either the cycle or on the branch. In this sense it would appear that the AAD molecule acts as a blocking group between the substructures even though it is itself intimately involved in both substructures. The highest frequency OH stretch vibration is more than 90% localized on the branch OH and appears at a frequency shifted only 8 $cm^{-1}$ from that of the donor methanol in the methanol dimer.

Whereas the normal modes of the cyclic trimer are highly delocalized around the ring, the asymmetrization produced by the binding of the branch to the cycle localizes the ring vibrations more than 80% on single OH groups (Table 4). This has two significant effects on the infrared spectra, first, in inducing intensity in the lowest frequency OH stretch vibration and, second, in breaking the near-degeneracy of the two high-frequency modes which carry all the intensity in the isolated cyclic trimer. Recent infrared spectra of benzene−$(H_2O)_3$ show precisely the same effect due to the asymmetry produced by benzene on the single-donor OH stretch vibrations of the water trimer.[66] Here the effect is enhanced due to the stronger H-bond formed by the branch methanol with the cyclic methanol trimer.

The recent matrix work of Coussan et al.[39] has identified a series of bands in the OH stretch region and assigned them to the (3) + 1 branched cycle tetramer. As Table 6 shows, the correspondence of the three observed bands (at a frequency shift of −162, −239, and −294 $cm^{-1}$) corresponds well with our calculated values of −158.9, −242.5, and −326.6 $cm^{-1}$, respectively, and lends some further confirmation to their assignment.

Similar effects of a branch are seen in the larger cycle present in (4) + 1; however, in that case the distortion is somewhat more localized, with the greatest effect on the branch-point methanol and lesser effects on the other three vibrations in the cyclic tetramer.

The OH stretch spectrum of the longer-branch (3) + 2 isomer can be interpreted roughly as the sum of a distorted cyclic trimer (3) and the D and AD molecules in the trimer chain 3. Again, the vibrations are largely localized on the cycle or branch, with "cross-talk" between the two substructures of only about 10%. The modes in the ring are quite localized due to the weakening of the 1→3 H-bond and the strengthening of the 3→2 H-bond upon branch formation.

Finally, the double-branched cyclic structure, (3) + 1 + 1, is notable in that four of the five H-bonds are to double-acceptor methanols (2→1, 5→1, 1→3, and 4→3). All four of these bonds are weak, and the vibrational frequency shifts of these vibrations fall between −145 and −233 $cm^{-1}$.

## V. Conclusions

In this paper, calculations of the structures, binding energies, vibrational frequencies, and infrared intensities of 13 low-energy conformations of $(CH_3OH)_n$ clusters with $n = 2-5$ have been presented. Analogous calculations on the lowest-energy structures of benzene−$(methanol)_n$, $n = 2$ and 3, have also been included and compared against new experimental resonant ion-dip infrared spectra.

An analysis of the calculated results has been given within the framework of four hydrogen-bonded structural types: cyclic, chain, branched-cyclic, and branched-chain. The cyclic and branched-cyclic $(CH_3OH)_n$ clusters maximize the number of H-bonds between methanol molecules, exceeding by one the number found in the chain and branched-chain structures of the same size. This, in combination with the increased cooperativity present in cyclic clusters, makes the cyclic clusters the global minimum structures for $n = 3-5$ and the branched cyclic clusters the next most stable structures for $n = 4$ and 5.

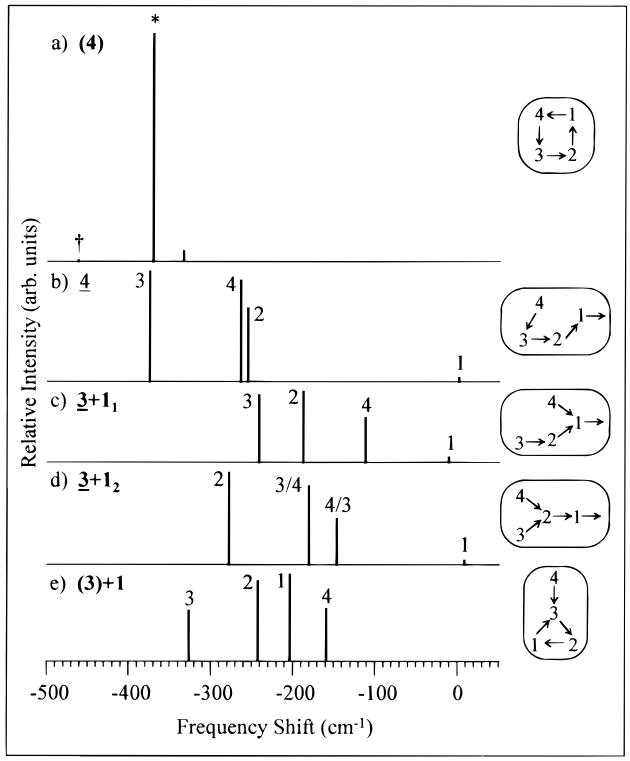


**Figure 6.** Stick diagram of the calculated OH stretch harmonic frequencies and infrared intensities for methanol tetramer (a) cycle (4), (b) chain (4), (c) branched chain 3 +$1_1$, d) branched chain 3 +$1_2$, and (e) branched cycle (3) + 1. The numbering on the vibrational transitions corresponds to the methanol numbering from Figures 1−4, and indicates which methanol OH has the largest coefficient(s) in that normal mode (Table 4). The inset summarizes the methanol numbering and direction of hydrogen donation in the hydrogen bonds.

An important goal of the present study has been the determination of the OH stretch spectral signatures for the various H-bonding topologies—cycles, chains, branched-cycles, and branched-chains. DFT calculations with the Becke3LYP functional and employing the 6-31+G* basis set produce OH stretch vibrational frequency shifts which match well with experimental values for $(methanol)_n$ and benzene−$(methanol)_n$ clusters in cases where a comparison can be made. The spectra calculated here confirm the OH stretch vibrations as a sensitive probe of the cluster's H-bonding structure, cooperativity, and intermolecular coupling. This is illustrated in Figure 6, where the calculated OH stretch spectra of five H-bonding topologies of the methanol tetramer are compared. Since these structures are representative of the 13 studied, we close by briefly highlighting their unique IR spectral characteristics.

Cyclic clusters such as the cyclic tetramer (4) (Figure 6a) carry all their OH stretch intensity in a nearly-degenerate pair of transitions with a large frequency downshift relative to the free OH of methanol monomer. The OH stretch vibrations are highly delocalized around the ring, bearing a correspondence with longitudinal phonons with different numbers of nodes in the phonon oscillation.[54]

H-bonded chains such as $\underline{4}$ (Figure 6b) have a free OH stretch which is hardly moved from its monomeric frequency. The other OH stretches are localized in large measure on a single OH group in the chain, as indicated in the figure. All the OH stretch bands carry intensity in the chain structures, but the interior methanols have an enhanced intensity which grows with increasing shift to lower frequency, as expected for OH stretch modes in increasingly strong H-bonds.

The spectral consequences of a branch in the branched-chain structures ($\underline{3} + 1_1$ and $\underline{3} + 1_2$) (Figure 6c,d) are similarly localized on a given OH group in the structure. The free OH stretch is once again present in the branched chains. However, the branched chains show generally smaller frequency shifts in their H-bonded OH stretches due to the weakening of the H-bonds to the branch-point methanol. The relative spacing of the H-bonded OH vibrations is also changed from that in the unbranched chain.

Finally, the branched cycles, represented by $(3) + 1$ (Figure 6e) have only H-bonded OH stretches, one near the donor OH of the methanol dimer and the other three near those of the cyclic methanol trimer. The asymmetry imposed by the branch on the trimer cycle partially localizes the vibrations in the cycle, turning on intensity in all its OH modes and breaking the near-degeneracy of the transitions within the cycle.

**Acknowledgment.** The authors gratefully acknowledge the support of the National Science Foundation (NSF CHE 9404716) for this work. They also thank Prof. K. Jordan of the University of Pittsburgh for his keen interest, helpful suggestions, and generous sharing of computer resources at a crucial stage of this project. The authors are also grateful to M. Yanez and P. Perchard for sharing their results prior to publication.

## References and Notes

(1) Gregory, J. K.; Clary, D. C. *J. Phys. Chem.* **1996**, *100*, 18014−18022.
(2) Millot, C.; Stone, A. J. *Mol. Phys.* **1992**, *77*, 439.
(3) Engkvist, O.; Forsberg, N.; Schutz, M.; Karlstrom, G. *Mol. Phys.* **1997**, *90*, 277−287.
(4) Pedulla, J. M.; Vila, F.; Jordan, K. D. *J. Chem. Phys.* **1996**, *105*, 11091.
(5) Buck, U.; Gu, X.; Lauenstein, C.; Rudolph, A. *J. Phys. Chem.* **1988**, *92*, 5561−62.
(6) Felker, P. M. *J. Phys. Chem.* **1992**, *96*, 7844.
(7) Felker, P. M. *Chem. Rev. (Washington, D.C.)* **1994**, *94*, 1784.
(8) Huisken, F.; Kaloudis, M.; Kulcke, A. *J. Chem. Phys.* **1996**, *104*, 17−25.
(9) Huang, Z. S.; Miller, R. E. *J. Chem. Phys.* **1989**, *91*, 6613−31.
(10) Nesbitt, D. J. *Chem. Rev.* **1988**, *88*, 843−70.
(11) Liu, K.; Gregory, J. K.; Brown, M. G.; Carter, C.; Saykally, R. J.; Clary, D. C. *Nature* **1996**, *381*, 501−503.
(12) Zwier, T. S. *Annu. Rev. Phys. Chem.* **1996**, *47*, 205−241.
(13) Xantheas, S. S.; Dunning, T. H., Jr. *J. Chem. Phys.* **1993**, *99*, 8774−92.
(14) Xantheas, S. S. *J. Chem. Phys.* **1994**, *100*, 7523.
(15) Chalasinski, G.; Rak, J.; Szczesniak, M. M.; Cybulski, S. M. *J. Chem. Phys.* **1997**, *106*, 3301−3310.
(16) VanDuijneveldt-Vanderijdt, J. G. C. M.; VanDuijneveldt, F. B. *Chem. Phys.* **1993**, *175*, 271−281.
(17) Schütz, M.; Klopper, W.; Luthi, H. P.; Leutwyler, S. *J. Chem. Phys.* **1996**, *103*, 6114−6126.
(18) vanderAvoird, A.; Olthof, E. H. T. *J. Chem. Phys.* **1996**, *105*, 8034−8050.
(19) Wales, D. J. *Science* **1996**, *271*, 925−929.
(20) Wales, D. J.; Walsh, T. R. *J. Chem. Phys.* **1997**, *106*, 7193−7207.
(21) Gregory, J. K.; Clary, D. C. *J. Chem. Phys.* **1996**, *105*, 6626−6633.
(22) Huisken, F.; Stemmler, M. *Chem. Phys. Lett.* **1988**, *144*, 391−95.
(23) Huisken, F.; Kulcke, A.; Laush, C.; Lisy, J. M. *J. Chem. Phys.* **1991**, *95*, 3924−29.
(24) Buck, U.; Ettischer, I. *J. Chem. Phys.* **1994**, *100*, 6974−76.
(25) Odutola, J. A.; Viswanathan, R.; Dyke, T. R. *J. Am. Chem. Soc.* **1979**, *101*, 4787−92.
(26) Kay, B. D.; Castleman, A. W. J. *J. Phys. Chem.* **1985**, *89*, 4867−68.
(27) Lovas, F. J.; Belov, S. P.; Tretyakov, M. Y.; Stahl, W.; Suenram, R. D. *J. Mol. Spectrosc.* **1995**, *170*, 478−92.
(28) Huisken, F.; Kaloudis, M.; Koch, M.; Werhahn, O. *J. Chem. Phys.* **1996**, *105*, 8965−8968.
(29) Dyke, T. R.; Mack, K. M.; Muenter, J. S. *J. Chem. Phys.* **1977**, *66*, 498−510.
(30) Odutola, J. A.; Dyke, T. R. *J. Chem. Phys.* **1980**, *72*, 5062−70.
(31) Fraser, G. T. *Int. Rev. Phys. Chem.* **1991**, *10*, 189−206.
(32) Pugliano, N.; Saykally, R. J. *Science* **1992**, *257*, 1937−40.
(33) Liu, K.; Elrod, M. J.; Loeser, J. G.; Cruzan, J. D.; Pugliano, N.; Brown, M. G.; Rzepio, J.; Saykally, R. J. *Faraday Discuss.* **1994**, *97*, 35−41.
(34) Liu, K.; Loeser, J. G.; Elrod, M. J.; Host, B. C.; Rzepiela, J. A.; Pugliano, N.; Saykally, R. J. *J. Am. Chem. Soc.* **1994**, *116*, 3507−3512.
(35) Buck, U.; Schmidt, B.; Siebers, J. G. *J. Chem. Phys.* **1993**, *99*, 9428−37.
(36) Pribble, R. N.; Hagemeister, F.; Zwier, T. S. *J. Chem. Phys.* **1997**, *106*, 2145−2157.
(37) Zwier, T. S. The Infrared spectroscopy of hydrogen-bonded clusters: Cycles, chains, cubes, and three-dimensional networks. In *Advances in Molecular Vibrations and Collision dynamics*; Bowman, J. M., Ed.; JAI Press: Greenwich, CT, 1997; Vol. 3, in press.
(38) Coussan, S.; Bakkas, N.; Loutellier, A.; Perchard, J. P.; Racine, S. *Chem. Phys. Lett.* **1994**, *217*, 123−29.
(39) Coussan, S.; Loutellier, A.; Perchard, J. P.; Racine, S.; Peremans, A.; Tadjeddine, A.; Zheng, W. Q. *J. Chem. Phys.* **1997**, *107*, 6526−6540.
(40) Anwander, E. H. S.; Probst, M. M.; Rode, B. M. *Chem. Phys.* **1992**, *166*, 341−60.
(41) Bizzarri, A.; Stolte, S.; Reuss, J.; Rijdt, J. G. C. M. V. D.-V. D.; Duijneveldt, F. B. V. *Chem. Phys.* **1990**, *143*, 423−35.
(42) Bleiber, A.; Sauer, J. *Chem. Phys. Lett.* **1995**, *238*, 243.
(43) Ugliengo, P.; Bleiber, A.; Garrone, E.; Sauer, J.; Ferrari, A. M. *Chem. Phys. Lett.* **1992**, *191*, 537.
(44) Williams, R. W.; Cheh, J. L.; Lowrey, A. H.; Weir, A. F. *J. Phys. Chem.* **1995**, *99*, 5299.
(45) Mo, O.; Yanez, M.; Elguero, J. *J. Chem. Phys.* **1997**, *107*, 3592−3601.
(46) Mo, O.; Yanez, M.; Elguero, J. *J. Mol. Struct.* **1994**, *314*, 73−81.
(47) Brink, G.; Glasser, L. *J. Comput. Chem.* **1982**, *3*, 219−26.
(48) Curtiss, L. A. *J. Chem. Phys.* **1977**, *67*, 1144−49.
(49) Luck, W. A. P.; Schrems, O. *J. Molec. Struct.* **1980**, *60*, 333.
(50) Martin, T. P.; Bergmann, T.; Wassermann, B. *Cluster Energy Surfaces*; D. Reidel: Dordrecht, 1987.
(51) Shivaglal, M. C.; Singh, S. *Int. J. Quantum Chem.* **1989**, *36*, 105−118.
(52) Zakharov, V. V.; Brodskaya, E. N. *Russ. J. Phys. Chem.* **1995**, *69*, 579−84.
(53) Buck, U.; Schmidt, B. *J. Chem. Phys.* **1993**, *98*, 9410−24.
(54) Buckingham, A. D. *Proc. R. Soc. London, Ser. A* **1958**, *248*, 169.
(55) Buckingham, A. D. *Proceedings of the Royal Society of London, Series A* **1960**, *255*, 32.
(56) Buckingham, A. D. *Trans. Faraday Soc.* **1960**, *56*, 753.
(57) Becke, A. D. *J. Chem. Phys.* **1993**, *98*, 5648.
(58) Lee, C.; Yang, W.; Parr, R. G. *Phys. Rev. B* **1988**, *37*, 785.
(59) Vosko, S. H.; Wilk, L.; Nusir, M. *Can. J. Phys.* **1980**, *58*, 1200.
(60) Frisch, M. J.; Trucks, G. W.; Schlegal, H. B.; Gill, P. M. W.; Johnson, B. G.; Wong, M. W.; Foresman, J. B.; Robb, M. A.; Head-Gordon, M.; Replogle, E. S.; Gomperts, R.; Andres, J. L.; Raghavachari, K.; Binkley, J. S.; Gonzalez, C.; Martin, R. L.; Fox, D. J.; Defrees, D. J.; Baker, J.; Stewart, J. J. P.; Pople, J. A. *Gaussian92 DFT Manual*; Gaussian, Inc.: Pittsburgh PA, 1993.
(61) Frisch, M. J.; Trucks, G. W.; Schlegel, H. B.; Gill, P. M. W.; Johnson, B. G.; Robb, M. A.; Cheeseman, J. R.; Keith, T. A.; Petersson, G. A.; Montgomery, J. A.; Raghavachari, K.; Al-Laham, M. A.; Zakrzewski, V. G.; Ortiz, J. V.; Foresman, J. B.; Cioslowki, J.; Stefanov, B. B.; Nanayakkara, A.; Challacombe, M.; Peng, C. Y.; Ayala, P. Y.; Chen, W.; Wong, M. W.; Andres, J. L.; Replogle, E. S.; Gomperts, R.; Martin, R. L.; Fox, D. J.; Binkley, J. S.; Defrees, D. J.; Baker, J.; Stewart, J. P.; Head-Gordon, M.; Gonzalez, C.; Pople, J. A. *Gaussian 94 (Revision A.1)*; Gaussian, Inc.: Pittsburgh PA, 1995.
(62) Clark, T.; Chandrasekhar, J.; Spitznagel, G. W.; P.v. R. SchleyerJ. Comput. Chem. 4. *J. Comput. Chem.* **1983**, *4*, 294.
(63) Hehre, W. J.; Ditchfield, R.; Pople, J. A. *J. Chem. Phys.* **1972**, *56*, 2257.
(64) Xantheas, S. S. *J. Chem. Phys.* **1995**, *102*, 4505−17.
(65) Estrin, D. A.; Paglieri, L.; Corongui, G.; Clementi, E. *J. Phys. Chem.* **1996**, *100*, 8701−8711.
(66) Fredericks, S.; Jordan, K. D.; Zwier, T. S. *J. Phys. Chem.* **1996**, *100*, 7810−7821.
(67) Fitzgerald, G.; Lee, C.; Chen, H. *J. Chem. Phys.* **1994**, *101*, 4472−4473.

(68) DelBene, J. E.; Person, W. B.; Szczepaniak, K. *J. Phys. Chem.* **1995**, *99*, 10705−10707.
(69) Novoa, J. J.; Sosa, C. *J. Phys. Chem.* **1995**, *99*, 15837−15845.
(70) Süle, P.; Nagy, A. *J. Chem. Phys.* **1996**, *104*, 8524−8534.
(71) Gonzalez, L.; Mo, O.; Yanez, M.; Elguero, J. *J. Mol. Struct.; THEOCHEM* **1996**, *371*, 1−10.
(72) Gruenloh, C. J.; Carney, J. R.; Arrington, C. A.; Zwier, T. S.; Fredericks, S. Y.; Jordan, K. D. *Science* **1997**, *276*, 1678.
(73) Gruenloh, C. J.; Hagemeister, F. C.; Carney, J. R.; Zwier, T. S. Unpublished results.
(74) Dunning, T. H. *J. Chem. Phys.* **1989**, *90*, 1007.
(75) Kendall, R. H.; Dunning, T. H.; Harrison, R. J. *J. Chem. Phys.* **1992**, *96*, 6796.
(76) Burgi, T.; Graf, S.; Leutwyler, S.; Klopper, W. *J. Chem. Phys.* **1995**, *103*, 1077−84.
(77) Honegger, E.; Leutwyler, S. *J. Chem. Phys.* **1988**, *88*, 2582−95.
(78) Boys, S. F.; Bernardi, F. *Mol. Phys.* **1970**, *19*, 553.
(79) Cooley, J. W. *Math. Comput.* **1961**, *15*, 163.
(80) Mo, O.; Yanez, M.; Elguero, J. *J. Chem. Phys.* **1992**, *97*, 6628−6638.